



HHS Public Access

Author manuscript

ACS Nano. Author manuscript; available in PMC 2023 May 19.

Published in final edited form as:

ACS Nano. 2023 April 25; 17(8): 7051–7063. doi:10.1021/acsnano.3c00536.

Optical Manipulation Heats up: Present and Future of Optothermal Manipulation

Pavana Siddhartha Kollipara,

Walker Department of Mechanical Engineering, The University of Texas at Austin, Austin, Texas 78712, United States

Zhihan Chen,

Materials Science and Engineering program and Texas Materials Institute, The University of Texas at Austin, Austin, Texas 78712, United States

Yuebing Zheng

Materials Science and Engineering program and Texas Materials Institute, The University of Texas at Austin, Austin, Texas 78712, United States

Abstract

Optothermal manipulation is a versatile technique that combines optical and thermal forces to control synthetic micro-/nanoparticles and biological entities. This emerging technique overcomes the limitations of traditional optical tweezers, including high laser power, photon and thermal damage to fragile objects, and the requirement of refractive-index contrast between target objects and the surrounding solvents. In this perspective, we discuss how the rich opto-thermo-fluidic multiphysics leads to a variety of working mechanisms and modes of optothermal manipulation in both liquid and solid media, underpinning a broad range of applications in biology, nanotechnology, and robotics. Moreover, we highlight current experimental and modeling challenges in the pursuit of optothermal manipulation and propose future directions and solutions to the challenges.

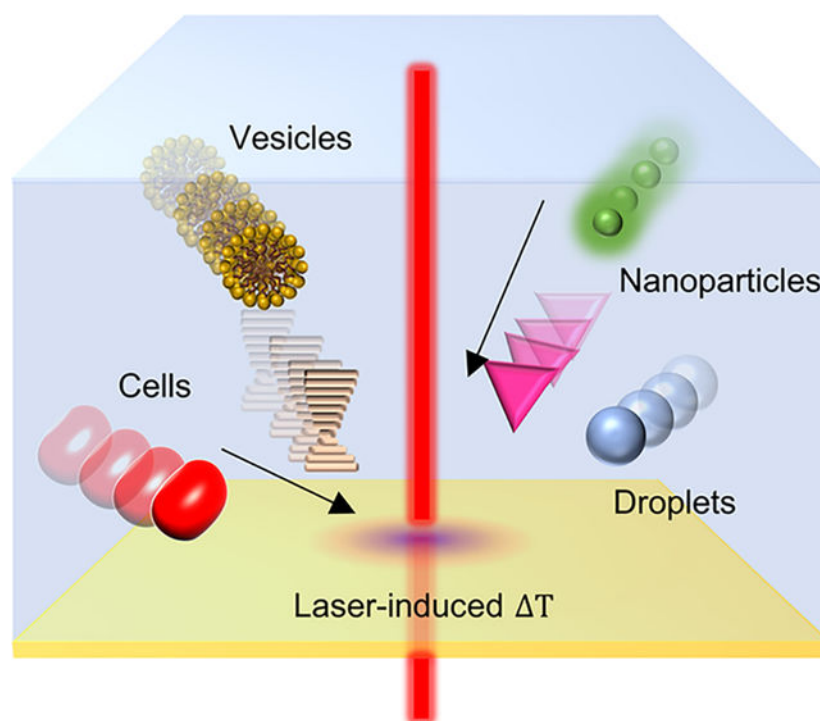
Graphical Abstract

Corresponding Author: Yuebing Zheng – zheng@austin.utexas.edu.

Author Contributions

P.S.K., Z.C., and Y.Z. framed the structure of the manuscript. P.S.K. and Y.Z. wrote the initial manuscript. All authors participated in the review and editing of the manuscript.

The authors declare no competing financial interest.



Keywords

optical manipulation; optothermal manipulation; thermophoresis; optical tweezers; Soret effect

1. INTRODUCTION

Optical tweezers have been developed to manipulate objects at the micro- and nanoscales, such as colloids, micelles, vesicles, DNA/RNA, cells, molecules, etc.^{1,2} These tweezers use light-induced gradient and scattering forces to trap objects at the focus spot and allow for spatial control in all three dimensions (3D) by changing the spot position. Because of their site selectivity and noncontact nature, optical tweezers have seen numerous applications in the fields of micro- and nano- fabrication, biomechanical analysis, cell-cell interactions, and optical spectroscopy.^{3,4} However, optical tweezers are inherently limited by the requirement of a refractive index contrast between the trapped entities and the surroundings. High laser powers are commonly needed to overcome this, especially for living cells whose refractive index contrast is minimal due to fluid exchange between the cells and their surroundings, which can cause severe photon and thermal damage to delicate biological objects.⁵

To overcome the challenges faced by optical tweezers, various additional energy fields have been utilized. The integration of optical tweezers with dielectrophoretic drift of particles has resulted in the emergence of optoelectronic tweezers.⁶ This technology involves projecting virtual electrodes onto photosensitive substrates to localize electric fields that enable the trapping and manipulation of nanoparticles. Furthermore, the integration of optical tweezers with microfluidics has greatly enhanced its throughput, leading to the development of optofluidic manipulation for high-throughput sorting and sensing applications.⁷ Another

development in this area is opto-acoustic tweezers, which use bubbles generated⁸ through laser heating to attract and manipulate biological cells. Additionally, plasmonic tweezers are used to focus laser beams onto nanostructures for local enhancement of electric fields, thereby increasing the trapping strength at lower laser power.⁹

Similarly, optothermal manipulation has been developed to tackle the challenges of conventional optical tweezers by combining optical forces with light-induced localized thermal forces, where a temperature gradient generated across the target objects is tailored for versatile control.^{10,11} The synergy between the optical forces and thermal forces enables the manipulation of micro- and nanoscale objects with 2–3 orders lower laser power than traditional optical tweezers, leading to reduced photon damage and easier operation.^{12,13} Moreover, different thermal forces arising from the opto-thermo-fluidic coupling enable extra manipulation modes (e.g., nudging, pulling, and rotation) of target objects in both liquids and solid media, which have been implemented in various applications.

In this perspective, we discuss the fundamental mechanisms underpinning various optothermal manipulation modes. Next, we highlight the diverse manipulation modes and applications of optothermal manipulation. Finally, we discuss the current challenges in implementing optothermal manipulation followed by our suggested solutions.

2. FUNDAMENTALS OF OPTOTHERMAL MANIPULATION

Optothermal manipulation works by using light-absorbing components (either particles or substrates) to convert incident light energy into localized thermal energy.¹⁰ This thermal energy is then diffused due to the thermal diffusivity of the surrounding media, creating a temperature gradient that is directed toward the light-absorbing components. The temperature gradient can span a much larger area (about 10–25 times larger) than the electromagnetic fields of the incident light, allowing for the manipulation of objects far away from the laser hot spot.¹⁴ The motions of various synthetic particles and biological objects have been regulated using these optothermal fields (Figure 1a).¹⁵

The key to optothermal manipulation is the thermophoretic response of the target object. Specifically, when the object is dispersed in liquid, it is stabilized by its interaction potential with the solvent, whose properties such as density, viscosity, and permittivity are often strongly affected by temperature.¹⁶ When the solvent is locally heated by laser absorption of the substrate or the particle itself, the object experiences a change in the interaction potential along with other phenomena such as fluid flow and pressure difference across the object. This causes the object to drift toward the thermal hot spot (thermophilic) or away from it (thermophobic) depending on the net change in interaction potential (Figure 1b). This is known as thermophoresis or the Ludwig–Soret effect. In this perspective, we refer thermophoresis as the overall response of the suspended objects to the temperature gradient (interaction potential change with temperature), containing all the factors that influence the particle's motion.¹⁷ Typically, there are two approaches to tailoring the thermophoretic response of objects, i.e., adjusting the components of solvent or using the thermally induced fluidic flows, which lead to the variable scenarios of thermophoresis.

Researchers can control the thermophoretic drift of particles by changing the composition of the solvent (e.g., by adding electrolytes, surfactants, or polymers).^{18,19} Fundamentally, under temperature gradients, the thermophoretic drift of added entities can result in concentration gradients or electric fields, which alters the thermophoretic behavior of the objects. For example, when polymers or macromolecules are added to the system, they respond to the temperature gradient much faster than micro-/nanoparticles due to their low size and inertia. The drift of polymers results in a concentration gradient, which causes the “thermo-depletion drift” of the objects (Figure 1c).¹⁴ The term thermo-depletion is also referred more commonly to the absence of polymers on a section of the object during polymer thermophoresis, typically due to additional steric effects when the object is close to a surface or another object.²⁰ Additionally, when electrolytes are added to the system, the cations and anions drift with different velocities, resulting in a spatial redistribution of ions, thus generating a macroscopic electric field across the object. The field interacts with the screened charge of the objects, leading to a “thermo-electric drift” (Figure 1d).²¹ The temperature gradient also distorts the Debye layer around the particle, which causes a hydrostatic pressure gradient around the particle due to a spatially varying salinity (total number of ions) within the Debye layer, driving the “thermo-osmotic drift” of the particle (Figure 1e). The phenomena “thermo-depletion” and “thermo-osmosis” appear similar, although the former is due to the concentration gradient of polymer beyond the Debye layer, while the latter is due to the salinity gradient within the Debye layer. However, since both effects are due to diffusion of entities in the solution, they are a subset of thermo-diffusion (a combination of thermo-osmosis and thermo-depletion).

Macroscopic fluid flows can be generated during the heating process regardless of the properties of suspended objects, which can be used for long-range and massive manipulation of various objects.²² When the solvent is heated, the local density of the solvent decreases due to the thermal expansion of the fluid. This causes the lighter fluid to rise and the heavier fluid to move into the vacuum created by the lighter fluid, which eventually results in a macroscopic fluidic flow called natural convection (also called as Rayleigh–Bénard convection, Figure 1f).²³ Additionally, when the thermal gradient occurs at liquid/air or liquid/liquid interfaces, the resultant surface tension gradient can cause a macroscopic flow known as the Marangoni flow, which can manipulate the particles on the interface.^{24,25} Since the surface tension gradient is caused by the temperature gradient, the Marangoni flow is referred to as “thermo-capillary” flow (Figure 1g).

Despite its promise in enabling versatile manipulations, a variety of force fields arising from the substrate, solvent, solute, and any electrolytes upon generation of a temperature gradient perplexes the fundamental understanding and control of the optothermal manipulation. For example, the analytical models for thermophoretic motion of particles arise from the steady-state assumption that the net flux of all entities under a temperature gradient in the system is zero.¹⁸ The corresponding equations mathematically represent that the ion flux vanishes due to the competing thermo-electric field, pressure gradients, inherent thermophoresis, and thermo-diffusion and are assumed to be valid for ions, molecules, and micro/nanoparticles. This holds true for one-dimensional temperature gradients typically used in thermophoretic studies, where the temperature gradients are of the order of 1–1000 K/mm.²⁶ However, in optothermal tweezers, the temperature gradient can vary significantly

within a small distance from the laser hotspot ($\sim 10\text{--}25\ \mu\text{m}$), with a magnitude of $10^4\text{--}10^5\ \text{K/mm}$,¹² which potentially invalidates the equation. According to our scaling analysis, the equation is valid for all ions and molecules at all concentrations down to the micromolar level, which proves that it is a continuous state of matter. We evaluate this number by considering a small differential volume unit of $1\ \mu\text{m}^3$ around the thermal hot spot. However, for surfactants that form nanoscale micelles, the continuity approximation is only valid for concentrations above $0.2\ \text{mM}$ above their critical micellar concentration. If the micelles have an aggregation number of 100, a $1\ \text{mM}$ surfactant concentration yields almost 6000 micelles in the differential volume, which can be approximated as a continuous state of matter. Since the micelles are a few nanometers in size, the equation is also valid for nanoparticles (of $\sim 10\ \text{nm}$) at high concentrations but is invalid for microparticles (including some types of cells) at any concentration. Therefore, other methods such as multiparticle collision dynamics²⁷ are required for an in-depth analysis of thermophoretic motion. Also, newer methods to integrate continuum models for ions and electrolytes and stochastic models for microparticles are required, which are discussed further in Challenges and Opportunities. As for the biological applications, there is a constant mass transfer between the cell and the extracellular fluid even at a constant temperature,²⁸ which results in thermal regulation of the cell. To fully understand the effects on the manipulation of biological cells, mass transfer analysis must be performed in conjunction with the above effects (e.g., thermophoresis, thermo-osmosis) to determine the cells' thermal drift directionality. Therefore, further research is necessary to develop more exhaustive models and force fields to better understand and estimate the thermophoretic drift.

3. DIVERSE OPTOTHERMAL MANIPULATION MODES

Since optothermal manipulation combines both optical and thermal forces, they can achieve capabilities similar to those of optical tweezers, where trapping and translational manipulation of target objects can be implemented in 3D. In addition, by tailoring the synergy of two types of forces, optothermal manipulation possesses a clear advantage in nudging and rotating capabilities over traditional optical tweezers. The expanded manipulation modes enable applications in nanomaterials, microrobotics, live 3D imaging, and biomechanical analysis.

For trapping and translational manipulation modes, optical tweezers have inherent limitations when it comes to trapping certain types of particles either due to the strong optical scattering force of the target particles or the requirement of the refractive index contrast. For example, metallic particles have a high scattering cross-section, which can result in the repulsion of particles due to high optical scattering force. To overcome this, beam-shaping techniques are often demanded to trap the particles in a local equilibrium state, complicating the optical setup.²⁹ In contrast, optothermal tweezers have been able to trap and manipulate more general types of objects by the design of solvents,³⁰ surfactants,³¹ or electrolytes³² with simple optics (Figure 2a,b). The trapping technique is extended to provide site-selective force to assemble a variety of colloidal particles into superstructures or metamaterials (Figure 2c,d).³³ Optothermal nudging can also be implemented by using the thermophobic nature of particles. Fränzl et al. realized the nudging behavior for multilaser-beam-based swimming applications (Figure 2e–g).³⁴ To overcome the limit of

two-dimensional (i.e., in-plane) optothermal manipulation due to the use of light-absorbing substrates, Lin et al. have successfully demonstrated the 3D optothermal manipulation using a light-absorbing particle (Figure 2h,i).³⁵ Briefly, the temperature gradient generated by the particle enables the thermoelectric field that guides the particle to the laser focus, which can be moved in all three dimensions. Asymmetric scattering particles are also used to break the 2D limit and enable the out-of-plane motion of the particles.³⁶ The light-absorbing particles can also serve as mobile heating sources to facilitate the 3D optothermal manipulation of other objects (including non-light-absorbing objects).^{35,37}

Rotational manipulation mode requires the altering of the force and energy landscape in the plane perpendicular to the vector connecting particle center and laser focus.^{40,41} While optical tweezers can achieve rotation of particles, they often require asymmetric particles⁴² or a dual counterpropagating beam.⁴³ Optothermal manipulation, on the other hand, can achieve the rotation of various particles with simple optics by integrating multiple optothermal forces on the particle.⁴⁴ The in-plane optothermal rotation can be induced by different thermal forces such as thermoelectricity or thermodiffusion (Figure 2j,k).^{38,45} As for more complicated out-of-plane rotation, Ding et al. successfully broke the symmetry of the particles by introducing the thermo-electrokinetic effects from the substrate and achieved a wide range of out-of-plane rotation of synthetic colloids and biological cells (Figure 2l,m) with a single laser beam.³⁹ The out-of-plane rotation with simple optics is promising for applications in 3D cell visualization, cell mechanics, and microsurgery.

4. TRANSLATING OPTOTHERMAL MANIPULATION FROM LIQUID MEDIA TO SOLID SUBSTRATES

Due to the inherent Brownian motion of particles in the liquid, the precision of optical manipulation is reduced, particularly when it comes to manipulating nanoscale entities. Recently, optothermal manipulation has been developed to operate on solid substrates, where precise manipulation of nanoparticles with spatial resolution down to ~80 nm has been achieved (Figure 3a).⁴⁶ Briefly, the particles are first distributed on a thin phase-changing material. Upon laser illumination on the particles, the surrounding material turns into a quasi-liquid state due to the heating of the particles (or the substrate), allowing for the directional motion of particles based on optical scattering forces and/or thermocapillary forces. By varying the laser power and particle–laser distance, the particles can be switched between translational (Figure 3a,b) and rotational (Figure 3c,d) motions. To be more specific, Figure 3a,b illustrates the process of using a laser beam to move 200 nm metallic particles on a solid surface via optothermally gated photon nudging. As the size of the particles decreases to 80 nm, thermo-capillary force will become dominant as gold nanoparticles start to be multifaceted.⁴⁷ When the laser–particle distance is kept within a specific range, the optical forces and thermocapillary forces meet a radial balance, where the particles reorient themselves and start rotating around the laser beam (Figure 3c,d). The study also shows that ultraspherical gold nanoparticles can occasionally exhibit a nudging effect similar to that shown in Figure 3a, indicating that the rotation is a result of the multifaceted nature of the particles.

Apart from in-plane manipulation on one substrate, particles have also been demonstrated to be transported vertically between two substrates by directing a high-powered laser on the particles, where the optothermal effects were able to overcome the adhesion of the particles to the substrate and launch them to a second substrate (Figure 3e,f).⁴⁸ The precise manipulation of particles on solid substrates results in a wider range of opportunities for innovations in nanomaterials and nanodevices.⁴⁹ To further improve the efficiency and speed of optothermal manipulation on solid substrates, the distance between the particle and laser beam should be precisely controlled. A feedback loop could be a possible solution to allowing for the on-demand translation and rotation of particles to achieve nanorobots on solid substrates. Additionally, the interactions between the particle and the phase-changing material need to be studied in more depth to fully understand the fundamentals of optothermal manipulation on solid surfaces.

5. APPLICATIONS OF OPTOTHERMAL MANIPULATION

Due to the reduced photon damage and the various operation modes, optothermal manipulation has been making significant strides in biological applications. For instance, optothermal rotation has recently been used to evaluate the binding kinetics of homogeneous and heterogeneous targeted cells, which also displays the potential to evaluate kinetics in native human extracellular fluids (Figure 4a).⁵⁰ Similarly, the 3D subsurface adhesion characteristics of cells are characterized by simultaneous trapping, manipulation, and rotation of target cells (Figure 4b).⁵¹ Both applications are difficult to achieve using conventional optical tweezers because of the requirement of a well-aligned, counterpropagating dual-laser-beam setup to incorporate rotational nonequilibrium and the potential photon damage. For *in vivo* applications of optothermal tweezers, Cui et al. have demonstrated the use of near-infrared (NIR) laser beams for higher penetration depth and effective biofilm removal, demonstrating the applicability of optothermal tweezers for photothermal therapy (Figure 4c).⁵² Moreover, optothermal manipulation has enabled ablation applications,⁵³ microsurgery,⁵⁴ cancer diagnostics,⁵⁵ and study of cell–cell communication.¹² Overall, existing optothermal manipulation is well suited for *in vitro* applications, which can utilize the advantages of a light-absorbing substrate. However, its further *in vivo* application is limited by the requirement of a heatconversion entity, where Janus particles are promising because of their rotational and translational capabilities within deep tissues, unlocked by NIR-based optothermal manipulation.

Optothermal manipulation has also been utilized for a variety of microrobotic applications, where particles act as ships on liquid interfaces or submarines in bulk liquids. The particles moving on the interface are driven by thermo-capillary or thermal expansion forces, while particles immersed in the bulk fluid are mainly manipulated by thermophoresis, thermodepletion, or thermoelectricity. For example, Zhao et al. achieved interfacial milliscale swimmers fueled by visible light using a thermally expanding hydrogel, enabling micro solar sails by imitating cilia-like motion (Figure 4d).⁵⁶ Peng et al. synergized optical and thermoelectric forces and torques to demonstrate opto-thermoelectric swimmers with precise direction control, where two laser beams were used to control transport and rotation, respectively (Figure 4e).³⁸ Optothermal rotators at a millimeter scale can be achieved by breaking the rotational symmetry of particles to generate the asymmetric temperature

gradient (Figure 4f).^{57,58} Moreover, by pushing multiple particles in parallel based on optothermal manipulation, numerous particles can move collectively to form swarm robotics or be used to investigate the collective motion occurring in nature (Figure 4g).⁵⁹

Optothermal manipulation has also exhibited tremendous advantages in microfabrication of customized colloidal clusters. Unlike optical tweezers, optothermal tweezers can be used to form stable superstructures from individual colloidal particles by utilizing depletion force arising from the nonuniform distributions of micelles or macromolecules within and outside the clusters, facilitating the bonding between multiple particles and leading to the formation of tunable metamaterials (Figure 4h).^{60,61} Moreover, the assembled superstructures can be reconfigurable because the micelles or macromolecules used to stabilize the structures can be controlled by the laser power to modulate the depletion force. The use of light-absorbing particles has the potential to form 3D metamaterials with an optothermal assembly. Additionally, gold particle assemblies created using optothermal tweezers have further been used in surface-enhanced Raman spectroscopy to improve the detection limit of Rhodamine 6G molecules in the solution (Figure 4i).^{62,63} While optical tweezers can also be used for this purpose, the higher scattering force limits the size of plasmonic particle assemblies, thereby reducing the Raman enhancement and the detection limit.

6. CHALLENGES AND OPPORTUNITIES

Despite decades of research on identifying the underlying mechanisms of thermophoresis, there are still severe limitations in the fundamental understanding and the future applications of optothermal manipulation. This is due to many uncontrollable, and sometimes unmeasurable, effects existing in the temperature-gradient liquid (or solid) system (e.g., hydrogen bonding in dual-component solvents). Moreover, laser-induced thermophoresis increases the complexity as the temperature gradient spatially varies in 3D. We delve into the simulation and experimental challenges that are required to be conquered to improve optothermal manipulation for a wider range of applications.

6.1. Atomistic Modeling Challenges of Optothermal Manipulation.

Simulating and modeling the thermal force fields of particles in solutions is challenging because of the influence of nanoscale effects such as interfacial charge distribution, which makes it difficult to accurately predict the thermophoretic response of a particle, thus hindering the fundamental understanding of optothermal manipulation. For example, changing the electrolyte from NaCl to NaOH can deterministically cause the polystyrene particles to change from thermophobic to thermophilic at ambient temperature due to a change in thermoelectric effect.²¹ However, in biocompatible solvents such as phosphate-buffered saline containing 90% NaCl, the thermophoretic response of living entities still remains difficult to estimate due to the response of several other ions in different concentrations in the solution. To address such challenges, molecular dynamics (MD) simulations are commonly used to study the thermal drifts of ions and estimate the Soret coefficients that determine their drift direction and velocity.⁶⁴ MD simulations involve modeling the interaction potential between atoms and molecules in the system and can give insights into system characteristics at the subnanometer scale. However, such simulations

are limited by computational cost and can only be applied to nanometer-sized domains with high pressure, high temperature gradient, and high concentrations of salt to observe a concentration gradient that helps visualize a thermoelectric potential difference (temperature gradients of the order of 10^9 K/m are required to observe a concentration change c of 2–5% within the nanometer scale simulation domains). In addition, MD simulations cannot be evaluated for the sufficient time required for equilibration, mainly due to the computation cost. Moreover, the evaluation of thermophoretic behavior is strongly dependent on the interaction potential models (force fields) used to simulate the atomic interactions, which involve several assumptions and might cause discrepancies between experiments and simulations.⁶⁵ Finally, MD simulations are only limited to ions and molecules, while nanoparticles and microparticles cannot be involved due to the size and cost constraints. In summary, while MD simulations have provided significant insights at the atomic level, due to their limitations, researchers prefer analytical models to understand the effects of thermophoresis.

6.2. Analytical Modeling Challenges of Optothermal Manipulation.

Analytical modeling is a process of using mathematical equations to solve the system's behavior, i.e., the response of the particles, ions, and surfactants in the solution to a temperature gradient between the nanometer to micrometer regime, by approximating the system to be a continuum media.⁶⁶ Such modeling techniques have led to an enormous understanding of thermophoretic mechanisms in the last two decades.^{67,68} However, the current models' usefulness in practical applications is still limited by certain assumptions and idealized scenarios, especially for the biological applications of optothermal manipulation.⁶⁹ For example, the temperature gradient in several derivations of thermal force fields is assumed to be a constant because the models have been developed for unidirectional thermal gradients. However, the assumption is invalid in spatially varying temperature gradients and in the case of light-absorbing particles. In addition, current models mostly treat particles as objects with smooth, nonpermeable surfaces, which cannot be implemented for cell thermophoresis, where different cells have different surface textures.⁷⁰ Moreover, water permeation across the cell membrane must be considered to accurately determine the thermophoretic response of the cell because water permeation is responsible for temperature regulation and cell dynamics with the extracellular fluid.^{71,72} Finally, additional structures on cell surfaces such as cilia or flagella might tune the thermophoretic response of the cells for which subsurface characteristics must be included in the analytical models, which is extremely challenging.⁷³

6.3. Integration of MD Simulations and Analytical Models for Optothermal Manipulation.

Newer approaches are required to automate the bridging of MD simulations and analytical models to solve for the multiscale nature of optothermal manipulation. Ideally, multiscale simulations must be performed by integrating MD simulations and analytical modeling to obtain particle–solvent interactions at the atomic scale and then translate the information into coarse-grained continuum models.^{74,75} Simultaneous validation of these models can be performed through experiments, but the controllable parameters in the experimental system are limited and the output is only the total thermal drift of the particle, which hardly helps to decouple the different contributions in optothermal tweezers.

Figure 5 illustrates the modeling framework that suggests the relationship between the tunable variables in the system to the opto-thermophoretic response of particles. The laser power, laser-particle distance, environmental temperature, and concentration of ions in the solution are the only four variables that can be adjusted. While it is possible to change the types of electrolytes or the laser wavelength to adjust the manipulation behavior, the solution (and sometimes the concentration) is restricted, especially in biological applications. Beyond the controllable variables, the thermophoretic response is also affected by multiple properties of the particle, the solvent, the electrolyte, and the surfactant.⁶⁷ Of these, several properties such as viscosity, density, and dissociation constants are temperature dependent as well.^{76–78} In particular, the properties of surfactants are highly influenced by temperature, as they can significantly alter the formation of micelles, resulting in changes in the aggregation number, critical micellar concentration, and the effective charge on the micelle.^{79,80} A recent work from Wenger's group clearly identifies the individual contributions of optical and thermophoretic forces and their effects on optothermal trapping using plasmonic double-nanohole apertures.⁸¹ The trapping stiffnesses vary strongly with laser power, concentration of the surfactant, and the type of surfactant used for trapping nanoparticles in their study.⁸¹ Additionally, new parameters such as Soret and Seebeck coefficients, Debye length, and ζ potential of the particle also play a role in determining the thermophoretic velocity of the particle, and these parameters depend on the prior properties and variables. While variables are tunable and properties can be obtained from the literature, these parameters must be derived analytically (Debye length, Seebeck coefficient) or obtained through experimental data (ζ potential, Soret coefficients). All variables, properties, and parameters together result in the evaluation of force fields, which requires strong analytical models to serve as links between properties and force fields. Finally, all forces together provide the thermophoretic velocity of the particle. Many modeling approaches assume that the temperature is a constant for property estimation, which is true for temperature variations across a spatial scale larger than the particle size but might lead to a significant cumulative error due to the presence of several parameters dependent on temperature in optothermal response evaluation. Therefore, to accurately describe force fields, it is necessary to consider the first-order approximation when the temperature changes.

6.4. Machine Learning as a Solution to Modeling Challenges of Optothermal Manipulation.

Machine learning offers a promising solution to the above modeling challenges, with minimal prior knowledge about the system and known parameter values (as mentioned in Figure 5).^{82,83} Machine-learning algorithms such as neural networks and support vector regression can be trained on data sets of known thermophoretic response of particles to predict the particle's response in new conditions. The intricate dependences among parameters, properties, and force fields can be overcome by the advantages of machine learning, which can treat the unknown dependences as a black box. Moreover, the nonlinearity of different differential equations used to model the response can easily be handled by machine-learning algorithms. With new advances in physics-based machine learning, the training and estimation can also be improved with minimal data as an input.^{84–86} Diverse machine learning models can be created at each length scale (mimicking both MD simulations and continuum models), which can be linked to accurately predict the

particles' response to an external temperature gradient at the microscale and simultaneously estimate the particle–solvent interactions down to the nanoscale.

6.5. Experimental Challenges and Opportunities of Optothermal Manipulation.

Beyond the simulation and analytical challenges, the realization and applications of optothermal manipulation are mainly limited by a couple of experimental challenges.

One is that most synthetic particles and biological objects are thermophobic at ambient temperature: i.e., they tend to move away from the laser hot spot. While such a motion is required for some of the swimming and robotic applications, thermophilic behavior is often required for biological study, microfabrication, and optical spectroscopy. To enable the optothermal trapping of different particles in all situations, researchers have used surfactants like CTAC to generate a thermoelectric field and simultaneously alter the particle surface charges.³¹ Recently, biocompatible surfactants have been studied to enable the trapping of cellular objects for biological applications, which does not alter the cell dynamics and cell–solvent and cell–cell interactions.⁸⁷ In opto-refrigerative tweezers, laser cooling is implemented to attract thermophobic particles to the laser focus with the lower temperature.⁸⁸ In several instances, protein complexes also demonstrate thermophobic behavior at all temperatures above 0 °C.⁸⁹ However, trapping biological entities at physiological temperatures is often essential to study their cellular interactions. The readers are directed toward a review article by Niether and Wiegand highlighting the complexity of thermophoresis in a biological context.⁶⁹ Additionally, techniques such as beam shaping and substrate design have been used to create ring-shaped optothermal potentials to encase hydrophobic objects in a laser-based heat barrier.⁹⁰ Such ring-shaped potentials can be effectively shaped such that the ring temperature of the enclosed domain can be maintained at physiological temperatures, while still enabling the thermophobic trapping.⁹¹ Such a mechanism has already been used to study the aggregation dynamics of proteins and amyloid fibers.⁹²

The other is that the enhanced temperature during optothermal manipulation increases the Brownian motion and destabilizes the particle in the trapping zone. Although optothermal tweezers on solid substrates arose as a promising solution, other techniques are essential to overcome the problem in liquid media. Plasmonic tweezers⁹³ offer the right combination of site specificity and controlled heat generation, which enables plasmon-enhanced optical or optothermal trapping along with optothermal delivery of target particles.^{94–98} Using plasmonic nanostructures as substrates, target particles are attracted from long-range distances and trapped locally and stably at the nanostructures due to the enhanced electromagnetic and temperature hot spots.^{97,99} The highly localized electric field enhancements lead to a high trapping stiffness of different entities such as DNA, proteins, nanoparticles, and quantum dots. Initial studies did not include the effects of thermophoretic force on particle trapping, mainly due to negligible thermophoretic force at the singularity. Later works highlighted the temperature increase for low-power excitation of plasmonic nanoapertures, which results in long-range attraction of the nanoscale entities.^{100–102} Although plasmonic tweezers demonstrate great potential in certain biological applications such as detection, sensing, and translocation dynamics,^{103–105} the rigid hot spot locations

cannot enable the manipulation of particles required for distinct applications such as assembly, fabrication, and cell-interaction studies.

Various new advancements implementing optothermal manipulation are possible by overcoming the limitations. Initially, there will be no necessity to conduct experiments in complicated circumstances. This assists in recognizing the necessary surfactants or electrolytes to accomplish a predetermined optothermal manipulation performance, such as trapping, nudging, or rotation. The utilization of multiscale models helps in comprehending nanoscale phenomena and their impact on macroscopic force fields, which ultimately allows for technology translation to biomedical applications at the industrial level. Additionally, detection of optothermally accumulated biomarkers would facilitate the diagnosis of distinct diseases and aid in the 3D characterization of cells. With low laser powers, heterogenetic cell–cell interactions in their natural solutions would be feasible, contingent on their surroundings.¹⁰⁶

With their broad manipulation modes and applications, optothermal tweezers have proven to be an alternative or complementary tool to conventional optical tweezers. They have improved functional capabilities in several applications. With the further advancements that overcome both modeling and experimental challenges, optothermal tweezers will become a go-to technique in diverse applications of biomedical research, drug delivery, spectroscopy, micro-/nanomanufacturing, and micro-/nanorobotics.

Funding

P.S.K., Z.C., and Y.Z. acknowledge the financial support of the National Institute of General Medical Sciences of the National Institutes of Health (R01GM146962) and National Science Foundation (ECCS-2001650).

REFERENCES

- (1). Lehmuskero A; Johansson P; Rubinsztein-Dunlop H; Tong L; Käll M Laser Trapping of Colloidal Metal Nanoparticles. *ACS Nano* 2015, 9 (4), 3453–3469. [PubMed: 25808609]
- (2). Maragò OM; Jones PH; Gucciardi PG; Volpe G; Ferrari A C. Optical trapping and manipulation of nanostructures. *Nat. Nanotechnol.* 2013, 8 (11), 807–819. [PubMed: 24202536]
- (3). Gao D; Ding W; Nieto-Vesperinas M; Ding X; Rahman M; Zhang T; Lim C; Qiu C-W Optical manipulation from the microscale to the nanoscale: fundamentals, advances and prospects. *Light: Science Applications* 2017, 6 (9), No. e17039. [PubMed: 30167291]
- (4). Favre-Bulle IA; Stilgoe AB; Scott EK; Rubinsztein-Dunlop H Optical trapping in vivo: theory, practice, and applications. *Nanophotonics* 2019, 8 (6), 1023–1040.
- (5). Bustamante CJ; Chemla YR; Liu S; Wang MD Optical tweezers in single-molecule biophysics. *Nature Reviews Methods Primers* 2021, 1 (1), 25.
- (6). Wu MC Optoelectronic tweezers. *Nat. Photonics* 2011, 5 (6), 322–324.
- (7). Fan X; White IM Optofluidic microsystems for chemical and biological analysis. *Nat. Photonics* 2011, 5 (10), 591–597. [PubMed: 22059090]
- (8). Xie Y; Zhao C; Zhao Y; Li S; Rufo J; Yang S; Guo F; Huang TJ Optoacoustic tweezers: a programmable, localized cell concentrator based on opto-thermally generated, acoustically activated, surface bubbles. *Lab Chip* 2013, 13 (9), 1772. [PubMed: 23511348]
- (9). Zhang Y; Min C; Dou X; Wang X; Urbach HP; Somekh MG; Yuan X Plasmonic tweezers: for nanoscale optical trapping and beyond. *Light: Science & Applications* 2021, 10 (1), 59.
- (10). Liu S; Lin L; Sun H-B Opto-Thermophoretic Manipulation. *ACS Nano* 2021, 15 (4), 5925–5943. [PubMed: 33734695]

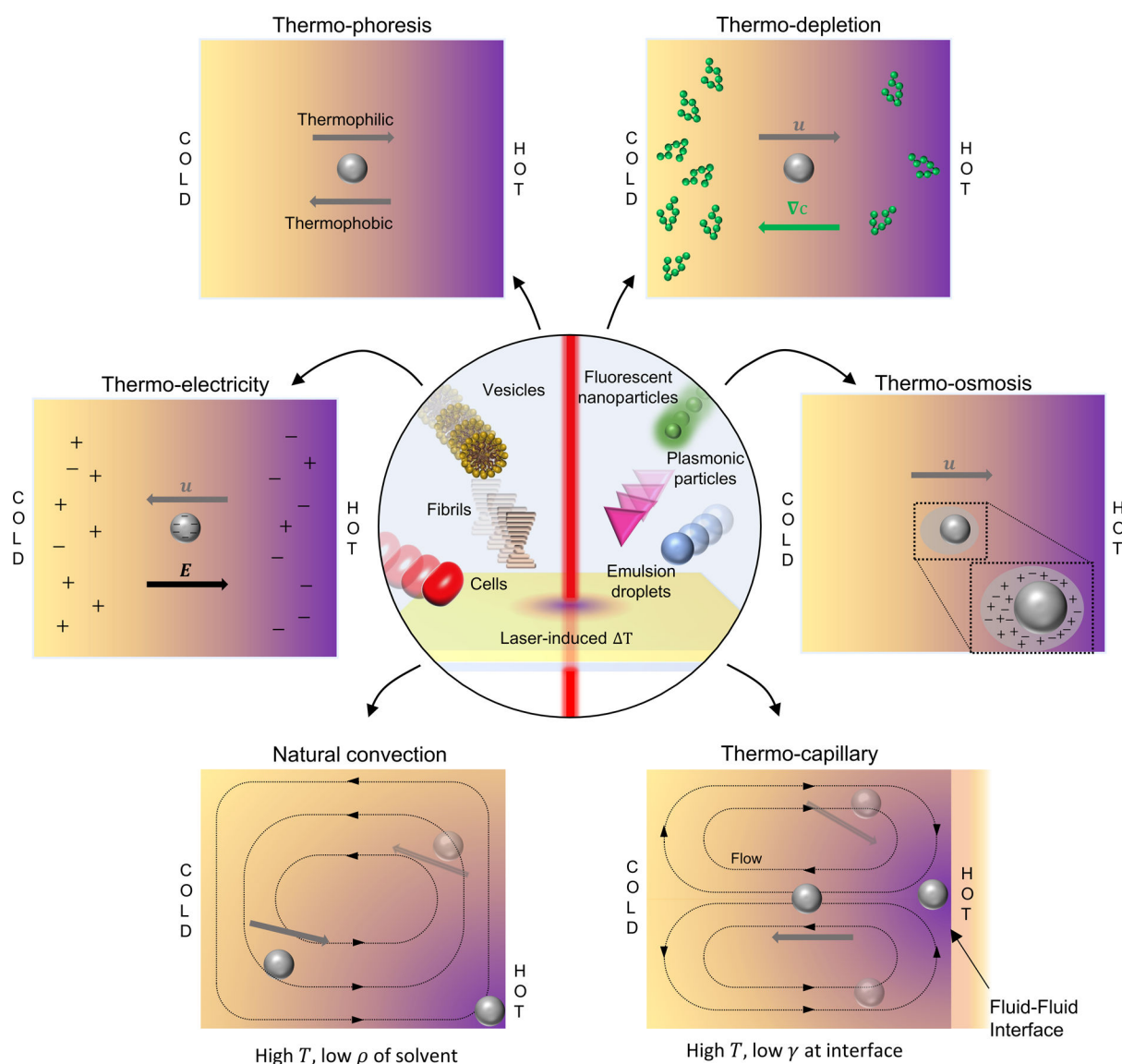
- (11). Chen Z; Li J; Zheng Y Heat-Mediated Optical Manipulation. *Chem. Rev.* 2022, 122 (3), 3122–3179. [PubMed: 34797041]
- (12). Lin L; Peng X; Wei X; Mao Z; Xie C; Zheng Y Thermophoretic Tweezers for Low-Power and Versatile Manipulation of Biological Cells. *ACS Nano* 2017, 11 (3), 3147–3154. [PubMed: 28230355]
- (13). Shao J; Abdelghani M; Shen G; Cao S; Williams DS; Van Hest JC M. Erythrocyte Membrane Modified Janus Polymeric Motors for Thrombus Therapy. *ACS Nano* 2018, 12 (5), 4877–4885. [PubMed: 29733578]
- (14). Jiang H-R; Wada H; Yoshinaga N; Sano M Manipulation of Colloids by a Nonequilibrium Depletion Force in a Temperature Gradient. *Phys. Rev. Lett.* 2009, 102 (20), 208301. [PubMed: 19519079]
- (15). Li J; Lin L; Inoue Y; Zheng Y Opto-Thermophoretic Tweezers and Assembly. *Journal of Micro and Nano-Manufacturing* 2018, 6 (4), 040801.
- (16). García-García S; Wold S; Jonsson M Effects of temperature on the stability of colloidal montmorillonite particles at different pH and ionic strength. *Appl. Clay Sci.* 2009, 43 (1), 21–26.
- (17). Piazza R Thermophoresis: moving particles with thermal gradients. *Soft Matter* 2008, 4 (9), 1740.
- (18). Vigolo D; Rusconi R; Stone HA; Piazza R Thermophoresis: microfluidics characterization and separation. *Soft Matter* 2010, 6 (15), 3489.
- (19). Lin L; Peng X; Zheng Y Reconfigurable opto-thermoelectric printing of colloidal particles. *Chem. Commun.* 2017, 53 (53), 7357–7360.
- (20). Edwards TD; Bevan MA Depletion-Mediated Potentials and Phase Behavior for Micelles, Macromolecules, Nanoparticles, and Hydrogel Particles. *Langmuir* 2012, 28 (39), 13816–13823. [PubMed: 22950666]
- (21). Würger A. Transport in Charged Colloids Driven by Thermoelectricity. *Phys. Rev. Lett.* 2008, 101 (10), 108302. [PubMed: 18851262]
- (22). Roxworthy BJ; Bhuiya AM; Vanka SP; Toussaint KC Understanding and controlling plasmon-induced convection. *Nat. Commun.* 2014, 5 (1), 3173. [PubMed: 24445431]
- (23). Jin CM; Lee W; Kim D; Kang T; Choi I Photothermal Convection Lithography for Rapid and Direct Assembly of Colloidal Plasmonic Nanoparticles on Generic Substrates. *Small* 2018, 14 (45), 1803055.
- (24). Lv C; Varanakkottu SN; Baier T; Hardt S Controlling the Trajectories of Nano/Micro Particles Using Light-Actuated Marangoni Flow. *Nano Lett.* 2018, 18 (11), 6924–6930. [PubMed: 30285458]
- (25). Dietrich K; Jaensson N; Buttinoni I; Volpe G; Isa L Microscale Marangoni Surfers. *Phys. Rev. Lett.* 2020, 125 (9), 098001. [PubMed: 32915612]
- (26). Lee N; Wiegand S Thermophoretic Micron-Scale Devices: Practical Approach and Review. *Entropy* 2020, 22 (9), 950. [PubMed: 33286719]
- (27). Yu N; Lou X; Chen K; Yang M Phototaxis of active colloids by self-thermophoresis. *Soft Matter* 2019, 15 (3), 408–414. [PubMed: 30565640]
- (28). Tang Y.-d.; Jin T; Flesch RCC. Effect of mass transfer and diffusion of nanofluid on the thermal ablation of malignant cells during magnetic hyperthermia. *Applied Mathematical Modelling* 2020, 83, 122–135.
- (29). Woerdemann M; Alpmann C; Esseling M; Denz C Advanced optical trapping by complex beam shaping. *Laser & Photonics Reviews* 2013, 7 (6), 839–854.
- (30). Peng X; Lin L; Hill EH; Kunal P; Humphrey SM; Zheng Y Optothermophoretic Manipulation of Colloidal Particles in Nonionic Liquids. *J. Phys. Chem. C* 2018, 122 (42), 24226–24234.
- (31). Lin L; Wang M; Peng X; Lissek EN; Mao Z; Scarabelli L; Adkins E; Coskun S; Unalan HE; Korgel BA; et al. Optothermoelectric nanotweezers. *Nat. Photonics* 2018, 12 (4), 195–201. [PubMed: 29785202]
- (32). Lin L; Peng X; Mao Z; Wei X; Xie C; Zheng Y Interfacial entropy-driven thermophoretic tweezers. *Lab Chip* 2017, 17 (18), 3061–3070. [PubMed: 28805878]

- (33). Lin L; Lepeshov S; Krasnok A; Jiang T; Peng X; Korgel BA; Alu A; Zheng Y All-optical reconfigurable chiral meta-molecules. *Mater. Today* 2019, 25, 10–20.
- (34). Fränzl M; Muiños-Landin S; Holubec V; Cichos F Fully Steerable Symmetric Thermoplasmonic Microswimmers. *ACS Nano* 2021, 15 (2), 3434–3440. [PubMed: 33556235]
- (35). Lin L; Kollipara PS; Kotnala A; Jiang T; Liu Y; Peng X; Korgel BA; Zheng Y Opto-thermoelectric pulling of light-absorbing particles. *Light: Science & Applications* 2020, 9 (1), 34.
- (36). Nedev S; Carretero-Palacios S; Kühler P; Lohmüller T; Urban AS; Anderson LJE; Feldmann J An Optically Controlled Microscale Elevator Using Plasmonic Janus Particles. *ACS Photonics* 2015, 2 (4), 491–496. [PubMed: 25950013]
- (37). Ghosh S; Ghosh A All optical dynamic nanomanipulation with active colloidal tweezers. *Nat. Commun.* 2019, 10 (1), 4191. [PubMed: 31519902]
- (38). Peng X; Chen Z; Kollipara PS; Liu Y; Fang J; Lin L; Zheng Y Opto-thermoelectric microswimmers. *Light: Science & Applications* 2020, 9 (1), 141.
- (39). Ding H; Kollipara PS; Kim Y; Kotnala A; Li J; Chen Z; Zheng Y Universal optothermal micro/nanoscale rotors. *Science Advances* 2022, 8 (24), No. eabn8498. [PubMed: 35704582]
- (40). Phillips DB; Padgett MJ; Hanna S; Ho YLD; Carberry DM; Miles MJ; Simpson SH Shape-induced force fields in optical trapping. *Nat. Photonics* 2014, 8 (5), 400–405.
- (41). Wang J; Xiong Z; Zheng J; Zhan X; Tang J Light-Driven Micro/Nanomotor for Promising Biomedical Tools: Principle, Challenge, and Prospect. *Acc. Chem. Res.* 2018, 51 (9), 1957–1965. [PubMed: 30179455]
- (42). Tanaka YY; Albella P; Rahmani M; Giannini V; Maier SA; Shimura T Plasmonic linear nanomotor using lateral optical forces. *Science Advances* 2020, 6 (45), No. eabc3726. [PubMed: 33148646]
- (43). Donato MG; Brzobohatý O; Simpson SH; Irrera A; Leonardi AA; Lo Faro MJ; Svak V; Maragò OM; Zemánek P Optical Trapping, Optical Binding, and Rotational Dynamics of Silicon Nanowires in Counter-Propagating Beams. *Nano Lett.* 2019, 19 (1), 342–352. [PubMed: 30525673]
- (44). Ding H; Chen Z; Ponce C; Zheng Y Optothermal rotation of micro-/nano-objects. *Chem. Commun.* 2023, 59 (16), 2208–2221.
- (45). Schmidt F; Magazzù A; Callegari A; Biancofiore L; Cichos F; Volpe G Microscopic Engine Powered by Critical Demixing. *Phys. Rev. Lett.* 2018, 120 (6), 068004. [PubMed: 29481280]
- (46). Li J; Liu Y; Lin L; Wang M; Jiang T; Guo J; Ding H; Kollipara PS; Inoue Y; Fan D Optical nanomanipulation on solid substrates via optothermally-gated photon nudging. *Nat. Commun.* 2019, 10 (1), 5672. [PubMed: 31831746]
- (47). Li J; Kollipara PS; Liu Y; Yao K; Liu Y; Zheng Y OptoThermocapillary Nanomotors on Solid Substrates. *ACS Nano* 2022, 16 (6), 8820–8826. [PubMed: 35594375]
- (48). Alam MS; Zhan Q; Zhao C Additive Opto-Thermomechanical Nanoprinting and Nanorepairing under Ambient Conditions. *Nano Lett.* 2020, 20 (7), 5057–5064. [PubMed: 32502352]
- (49). Li J; Wang M; Wu Z; Li H; Hu G; Jiang T; Guo J; Liu Y; Yao K; Chen Z; et al. Tunable Chiral Optics in All-Solid-Phase Reconfigurable Dielectric Nanostructures. *Nano Lett.* 2021, 21 (2), 973–979. [PubMed: 33372805]
- (50). Liu Y; Ding H; Li J; Lou X; Yang M; Zheng Y Light-driven single-cell rotational adhesion frequency assay. *eLight* 2022, 2 (1), 13. [PubMed: 35965781]
- (51). Ding H; Chen Z; Kollipara PS; Liu Y; Kim Y; Huang S; Zheng Y Programmable Multimodal Optothermal Manipulation of Synthetic Particles and Biological Cells. *ACS Nano* 2022, 16 (7), 10878–10889. [PubMed: 35816157]
- (52). Cui T; Wu S; Sun Y; Ren J; Qu X Self-Propelled Active Photothermal Nanoswimmer for Deep-Layered Elimination of Biofilm In Vivo. *Nano Lett.* 2020, 20 (10), 7350–7358. [PubMed: 32856923]
- (53). Joby JP; Das S; Pinapati P; Rogez B; Baffou G; Tiwari DK; Cherukulappurath S Optically-assisted thermophoretic reversible assembly of colloidal particles and *E. coli* using graphene oxide microstructures. *Sci. Rep.* 2022, 12 (1), 3657. [PubMed: 35256647]

- (54). He W; Frueh J; Hu N; Liu L; Gai M; He Q Guidable Thermophoretic Janus Micromotors Containing Gold Nanocolorifiers for Infrared Laser Assisted Tissue Welding. *Advanced Science* 2016, 3 (12), 1600206. [PubMed: 27981009]
- (55). Liu C; Zhao J; Tian F; Cai L; Zhang W; Feng Q; Chang J; Wan F; Yang Y; Dai B; et al. Low-cost thermophoretic profiling of extracellular-vesicle surface proteins for the early detection and classification of cancers. *Nature Biomedical Engineering* 2019, 3 (3), 183–193.
- (56). Zhao Y; Xuan C; Qian X; Alsaid Y; Hua M; Jin L; He X Soft phototactic swimmer based on self-sustained hydrogel oscillator. *Science Robotics* 2019, 4 (33), No. eaax7112. [PubMed: 33137784]
- (57). Maggi C; Saglimbeni F; Dipalo M; De Angelis F; Di Leonardo R Micromotors with asymmetric shape that efficiently convert light into work by thermocapillary effects. *Nat. Commun.* 2015, 6 (1), 7855. [PubMed: 26220862]
- (58). Meng F; Hao W; Yu S; Feng R; Liu Y; Yu F; Tao P; Shang W; Wu J; Song C; et al. Vapor-Enabled Propulsion for Plasmonic Photothermal Motor at the Liquid/Air Interface. *J. Am. Chem. Soc.* 2017, 139 (36), 12362–12365. [PubMed: 28837327]
- (59). Lavergne FA; Wendehenne H; Bäuerle T; Bechinger C Group formation and cohesion of active particles with visual perception–dependent motility. *Science* 2019, 364 (6435), 70–74. [PubMed: 30948548]
- (60). Lin L; Zhang J; Peng X; Wu Z; Coughlan ACH; Mao Z; Bevan MA; Zheng Y Opto-thermophoretic assembly of colloidal matter. *Science Advances* 2017, 3 (9), No. e1700458. [PubMed: 28913423]
- (61). Peng X; Li J; Lin L; Liu Y; Zheng Y Opto-Thermophoretic Manipulation and Construction of Colloidal Superstructures in Photocurable Hydrogels. *ACS Applied Nano Materials* 2018, 1 (8), 3998–4004. [PubMed: 31106296]
- (62). Tiwari S; Khandelwal U; Sharma V; Kumar GVP Single Molecule Surface Enhanced Raman Scattering in a Single Gold Nanoparticle-Driven Thermoplasmonic Tweezer. *J. Phys. Chem. Lett.* 2021, 12 (49), 11910–11918. [PubMed: 34878793]
- (63). Lin L; Peng X; Wang M; Scarabelli L; Mao Z; Liz-Marzán LM; Becker MF; Zheng Y Light-Directed Reversible Assembly of Plasmonic Nanoparticles Using Plasmon-Enhanced Thermophoresis. *ACS Nano* 2016, 10 (10), 9659–9668. [PubMed: 27640212]
- (64). Rezende Franco L; Sehnem AL; Figueiredo Neto AM; Coutinho K Molecular Dynamics Approach to Calculate the Thermodiffusion (Soret and Seebeck) Coefficients of Salts in Aqueous Solutions. *J. Chem. Theory Comput.* 2021, 17 (6), 3539–3553. [PubMed: 33942620]
- (65). Di Lecce S; Albrecht T; Bresme F The role of ion-water interactions in determining the Soret coefficient of LiCl aqueous solutions. *Phys. Chem. Chem. Phys.* 2017, 19 (14), 9575–9583. [PubMed: 28345697]
- (66). Vigolo D; Buzzaccaro S; Piazza R Thermophoresis and Thermoelectricity in Surfactant Solutions. *Langmuir* 2010, 26 (11), 7792–7801. [PubMed: 20146491]
- (67). Würger A Thermal non-equilibrium transport in colloids. *Rep. Prog. Phys.* 2010, 73, 126601.
- (68). Chen Z; Kollipara PS; Ding H; Pughazhendi A; Zheng Y Liquid Optothermoelectrics: Fundamentals and Applications. *Langmuir* 2021, 37 (4), 1315–1336. [PubMed: 33410698]
- (69). Niether D; Wiegand S Thermophoresis of biological and biocompatible compounds in aqueous solution. *J. Phys.: Condens. Matter* 2019, 31, 503003. [PubMed: 31491783]
- (70). Fischer EG Nuclear Morphology and the Biology of Cancer Cells. *Acta Cytologica* 2020, 64 (6), 511–519. [PubMed: 32570234]
- (71). Ferdinandus; Suzuki M; Vu CQ; Harada Y; Sarker SR; Ishiwata SI; Kitaguchi T; Arai S Modulation of Local Cellular Activities using a Photothermal Dye-Based Subcellular-Sized Heat Spot. *ACS Nano* 2022, 16 (6), 9004–9018. [PubMed: 35675905]
- (72). Tirza G; Solodeev I; Sela M; Greenberg I; Pasmanik-Chor M; Gur E; Shani N Reduced culture temperature attenuates oxidative stress and inflammatory response facilitating expansion and differentiation of adipose-derived stem cells. *Stem Cell Research & Therapy* 2020, 11 (1), 35. [PubMed: 31973743]
- (73). Gilpin W; Bull MS; Prakash M The multiscale physics of cilia and flagella. *Nature Reviews Physics* 2020, 2 (2), 74–88.

- (74). Belkin M; Chao S-H; Giannetti G; Aksimentiev A Modeling thermophoretic effects in solid-state nanopores. *Journal of Computational Electronics* 2014, 13 (4), 826–838. [PubMed: 25395899]
- (75). Belkin M; Maffeo C; Wells DB; Aksimentiev A Stretching and Controlled Motion of Single-Stranded DNA in Locally Heated Solid-State Nanopores. *ACS Nano* 2013, 7 (8), 6816–6824. [PubMed: 23876013]
- (76). Agar JN; Mou CY; Lin JL Single-ion heat of transport in electrolyte solutions: a hydrodynamic theory. *J. Phys. Chem.* 1989, 93 (5), 2079–2082.
- (77). Ewell RH; Eyring H Theory of the Viscosity of Liquids as a Function of Temperature and Pressure. *J. Chem. Phys.* 1937, 5 (9), 726–736.
- (78). Mallamace F; Branca C; Broccio M; Corsaro C; Mou C-Y; Chen S-H The anomalous behavior of the density of water in the range $30\text{ K} < T < 373\text{ K}$. *Proc. Natl. Acad. Sci. U. S. A.* 2007, 104 (47), 18387–18391. [PubMed: 18000049]
- (79). Malliaris A; Le Moigne J; Sturm J; Zana R Temperature dependence of the micelle aggregation number and rate of intramicellar excimer formation in aqueous surfactant solutions. *J. Phys. Chem.* 1985, 89 (12), 2709–2713.
- (80). Mehta SK; Bhasin KK; Chauhan R; Dham S Effect of temperature on critical micelle concentration and thermodynamic behavior of dodecyltrimethylammonium bromide and dodecyltrimethylammonium chloride in aqueous media. *Colloids Surf., A* 2005, 255 (1), 153–157.
- (81). Jiang Q; Rogez B; Claude J-B; Baffou G; Wenger J Quantifying the Role of the Surfactant and the Thermophoretic Force in Plasmonic Nano-optical Trapping. *Nano Lett.* 2020, 20 (12), 8811–8817. [PubMed: 33237789]
- (82). Zheng Y; Wu Z, Ed.; *Intelligent Nanotechnology: Merging Nanoscience and Artificial Intelligence*; 1st ed.; Elsevier Science: 2022; Vol. 1, pp 1–416.
- (83). Yao K; Zheng Y *Nanophotonics and Machine Learning*; 1st ed.; Springer: 2023; Vol. 1, pp 1–178. DOI: 10.1007/978-3-031-20473-9.
- (84). Dulaney AR; Brady JF Machine learning for phase behavior in active matter systems. *Soft Matter* 2021, 17 (28), 6808–6816. [PubMed: 34223598]
- (85). Cichos F; Gustavsson K; Mehlig B; Volpe G Machine learning for active matter. *Nature Machine Intelligence* 2020, 2 (2), 94–103.
- (86). Yao K; Unni R; Zheng Y Intelligent nanophotonics: merging photonics and artificial intelligence at the nanoscale. *Nanophotonics* 2019, 8 (3), 339–366. [PubMed: 34290952]
- (87). Ding H; Kollipara PS; Lin L; Zheng Y Atomistic modeling and rational design of optothermal tweezers for targeted applications. *Nano Research* 2021, 14 (1), 295–303. [PubMed: 35475031]
- (88). Li J; Chen Z; Liu Y; Kollipara PS; Feng Y; Zhang Z; Zheng Y Opto-refrigerative tweezers. *Science Advances* 2021, 7 (26), No. eabh1101. [PubMed: 34172454]
- (89). Wolff M; Mittag JJ; Herling TW; Genst ED; Dobson CM; Knowles TPJ; Braun D; Buell AK Quantitative thermophoretic study of disease-related protein aggregates. *Sci. Rep.* 2016, 6 (1), 22829. [PubMed: 26984748]
- (90). Braun M; Cichos F Optically Controlled Thermophoretic Trapping of Single Nano-Objects. *ACS Nano* 2013, 7 (12), 11200–11208. [PubMed: 24215133]
- (91). Braun M; Bregulla AP; Günther K; Mertig M; Cichos F Single Molecules Trapped by Dynamic Inhomogeneous Temperature Fields. *Nano Lett.* 2015, 15 (8), 5499–5505. [PubMed: 26161841]
- (92). Fränzl M; Thalheim T; Adler J; Huster D; Posseckardt J; Mertig M; Cichos F Thermophoretic trap for single amyloid fibril and protein aggregation studies. *Nat. Methods* 2019, 16 (7), 611–614. [PubMed: 31235884]
- (93). Pang Y; Gordon R Optical Trapping of 12 nm Dielectric Spheres Using Double-Nanoholes in a Gold Film. *Nano Lett.* 2011, 11 (9), 3763–3767. [PubMed: 21838243]
- (94). Kotnala A; Ding H; Zheng Y Enhancing Single-Molecule Fluorescence Spectroscopy with Simple and Robust Hybrid Nanoapertures. *ACS Photonics* 2021, 8 (6), 1673–1682. [PubMed: 35445142]
- (95). Peng X; Kotnala A; Rajeeva BB; Wang M; Yao K; Bhatt N; Penley D; Zheng Y Plasmonic Nanotweezers and Nanosensors for Point-of-Care Applications. *Advanced Optical Materials* 2021, 9 (13), 2100050. [PubMed: 34434691]

- (96). Kotnala A; Kollipara PS; Zheng Y Opto-thermoelectric speckle tweezers. *Nanophotonics* 2020, 9 (4), 927–933. [PubMed: 34290954]
- (97). Kotnala A; Kollipara PS; Li J; Zheng Y Overcoming Diffusion-Limited Trapping in Nanoaperture Tweezers Using Opto-Thermal-Induced Flow. *Nano Lett.* 2020, 20 (1), 768–779. [PubMed: 31834809]
- (98). Kotnala A; Zheng Y Opto-thermophoretic fiber tweezers. *Nanophotonics* 2019, 8 (3), 475–485. [PubMed: 34290953]
- (99). Liu Y; Lin L; Bangalore Rajeeva B; Jarrett JW; Li X; Peng X; Kollipara P; Yao K; Akinwande D; Dunn AK; et al. Nanoradiator-Mediated Deterministic Opto-Thermoelectric Manipulation. *ACS Nano* 2018, 12 (10), 10383–10392. [PubMed: 30226980]
- (100). Jiang Q; Rogez B; Claude J-B; Baffou G; Wenger J Temperature Measurement in Plasmonic Nanoapertures Used for Optical Trapping. *ACS Photonics* 2019, 6 (7), 1763–1773.
- (101). Xu Z; Song W; Crozier KB Direct Particle Tracking Observation and Brownian Dynamics Simulations of a Single Nanoparticle Optically Trapped by a Plasmonic Nanoaperture. *ACS Photonics* 2018, 5 (7), 2850–2859.
- (102). Verschuere DV; Pud S; Shi X; De Angelis L; Kuipers L; Dekker C Label-Free Optical Detection of DNA Translocations through Plasmonic Nanopores. *ACS Nano* 2019, 13 (1), 61–70. [PubMed: 30512931]
- (103). Keyser UF; Koeleman BN; Van Dorp S; Krapf D; Smeets RMM; Lemay SG; Dekker NH; Dekker C Direct force measurements on DNA in a solid-state nanopore. *Nat. Phys.* 2006, 2 (7), 473–477.
- (104). Spitzberg JD; Zrehen A; Van Kooten XF; Meller A Plasmonic-Nanopore Biosensors for Superior Single-Molecule Detection. *Adv. Mater.* 2019, 31 (23), 1900422.
- (105). Shi X; Verschuere DV; Dekker C Active Delivery of Single DNA Molecules into a Plasmonic Nanopore for Label-Free Optical Sensing. *Nano Lett.* 2018, 18 (12), 8003–8010. [PubMed: 30460853]
- (106). Armingol E; Officer A; Harismendy O; Lewis NE Deciphering cell-cell interactions and communication from gene expression. *Nat. Rev. Genet.* 2021, 22 (2), 71–88. [PubMed: 33168968]

**Figure 1.**

Overview and fundamental mechanisms of optothermal manipulation (a) Schematic of typical optothermal manipulation with light-absorbing substrates showing the control of diverse particles (fluorescent nanoparticles, plasmonic particles, emulsion droplets) and biological entities (cells, vesicles, DNA, fibrils). (b) Thermophoresis is the inherent drift of an object in a temperature gradient. If the object moves to the hot (cold), then it is called thermophilic (thermophobic). (c) Thermo-depletion occurs in the presence of an external polymer within the solution, which creates a concentration gradient under a temperature gradient. (d) Thermo-electricity is the macroscopic electric field (E , e.g., directed toward the hot) generated by the different drift of counterions in a temperature gradient. The resultant electric field interacts with the screened charge of the object (e.g., negative charge) and results in the object's drift (e.g., toward the cold). (e) Thermo-osmosis occurs when the charged Debye layer experiences a deformation due to the temperature gradient. The local concentration of ions (salinity) varies within the Debye layer, which causes a hydrostatic

pressure difference across the object. (f) Natural convection occurs when the temperature gradient causes a bulk fluid density (ρ) difference and results in a macroscopic flow. (g) Thermo-capillary flow occurs when the temperature gradient occurs at the interface of two immiscible fluids. γ indicates the surface tension.

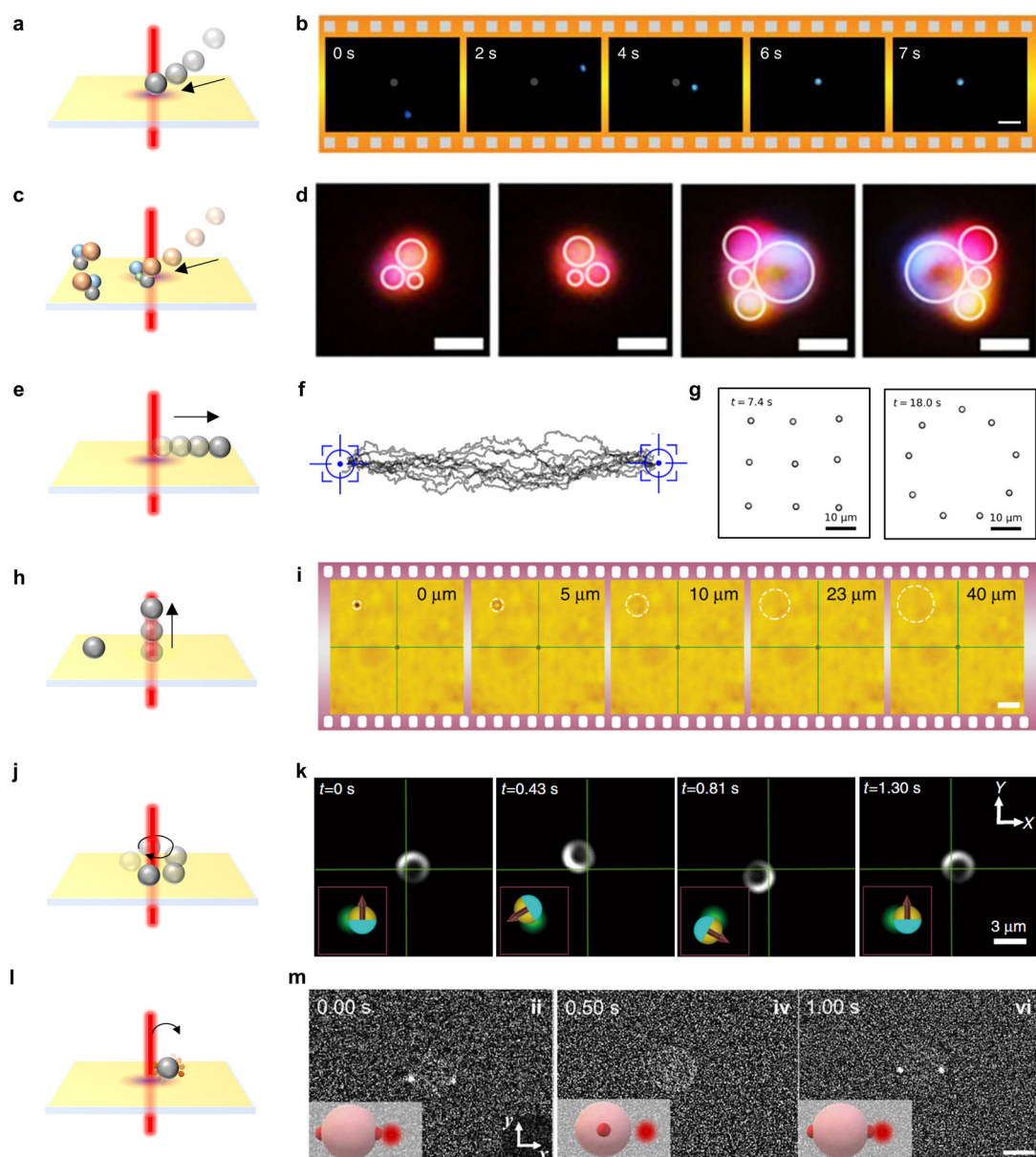


Figure 2.

Modes of optothermal manipulation in liquids (a, b) Schematic and time-lapse images of a particle getting attracted and trapped at the laser beam. Adapted with permission from ref 31. Copyright 2018 Springer Nature. (c, d) Schematic and time-lapse images of translating particles in-plane (on substrate) and creating diverse superstructures with various colloidal particles as building blocks. Adapted with permission from ref 33. Copyright 2019 Elsevier. (e) Schematic of particle nudging by the laser beam. (f) Trajectory of a single particle nudged between two distinct points. (g) Schematic of particle arrangement before and after nudging manipulation using multiple laser beams. Adapted with permission from ref 34. Copyright 2021 American Chemical Society. (h, i) Schematic and time-lapse images of translating light-absorbing particles out of plane (perpendicular to substrate). Adapted with permission under a Creative Commons CC BY License from ref 35. Copyright 2020

Springer Nature. (j, k) Schematic and time-lapse images of in-plane rotation of particles. Adapted with permission under a Creative Commons CC BY License from ref 38. Copyright 2020 Springer Nature. (l, m) Schematic and time-lapse images of out-of-plane rotation of particles; From ref 39. Copyright The Authors, some rights reserved; exclusive licensee American Association for the Advancement of Science. Distributed under a CC BY-NC 4.0 license. Reprinted with permission from American Association for the Advancement of Science. The temperature gradient is generated by light-absorbing substrates in (a, c, l), while the temperature gradient is generated by light-absorbing particles in (e, h, j). Scale bars: 10 μm (b, i), 1 μm (d), 2 μm (m).

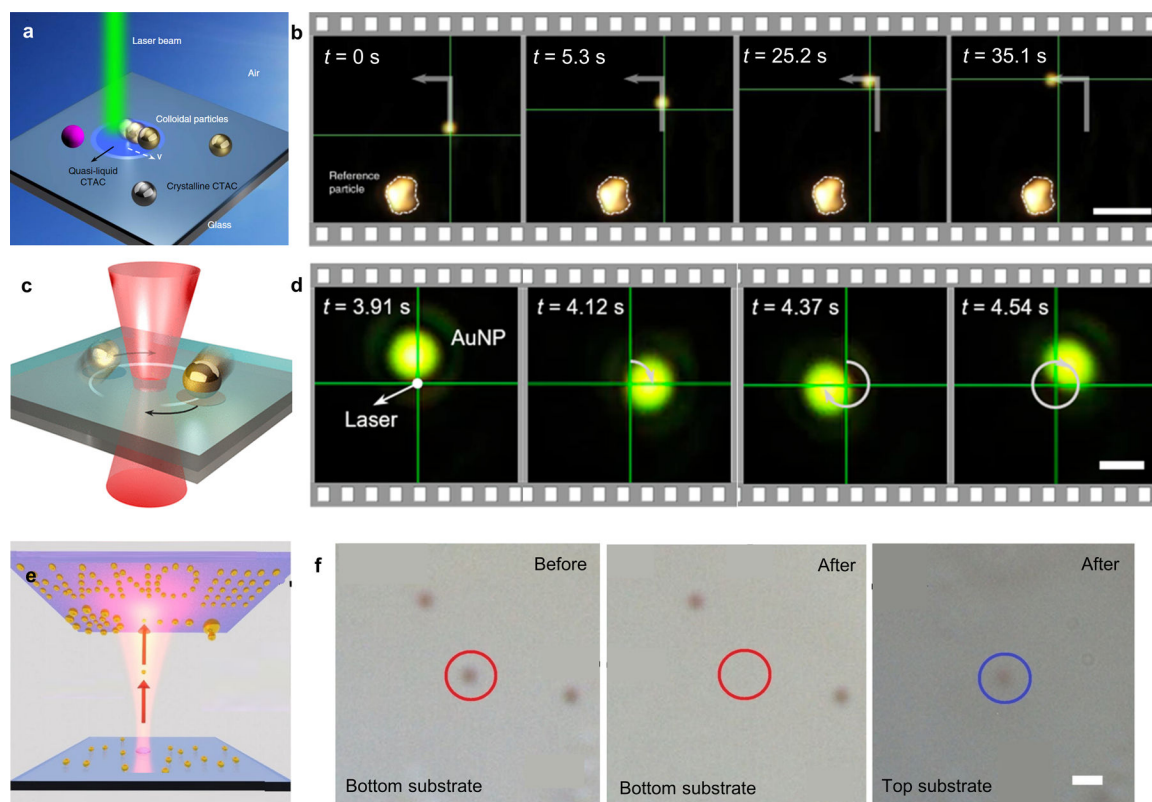


Figure 3. Optothermal manipulation beyond liquid media Schematic and microscopic images of (a, b) particles being nudged by the laser beam on the solid substrate; Adapted with permission under a Creative Commons CC BY License from ref 46. Copyright 2019 Springer Nature. (c, d) Particles rotating around the laser beam on the solid substrate Adapted with permission from ref 47. Copyright 2022 American Chemical Society. (e, f) Particles shot from the bottom substrate to the top substrate. Adapted with permission from ref 48. Copyright 2020 American Chemical Society. Scale bars: $5 \mu\text{m}$ (b), $1 \mu\text{m}$ (d), 500 nm (f).

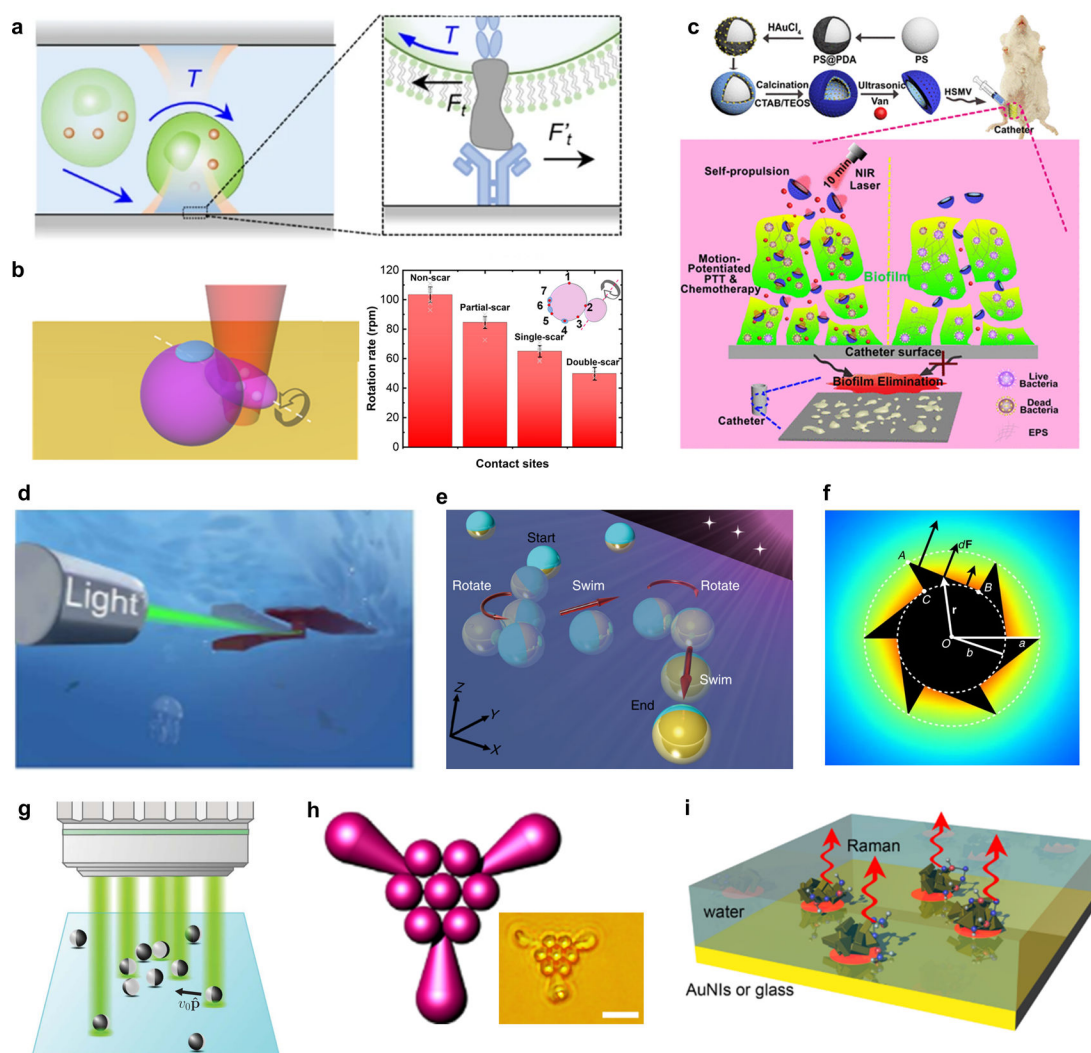


Figure 4.

Applications of optothermal manipulation (a, b) Cells are trapped and rotated out of plane to measure the shear adhesion kinetics between (a) cell and substrate, adapted with permission under a Creative Commons CC BY License from ref 50, copyright 2022 Springer Open, and (b) cell and cell, adapted with permission from ref 51, copyright 2022 American Chemical Society. (c) Schematic of optothermal-driven particles for biofilm removal. Adapted with permission from ref 52. Copyright 2020 American Chemical Society. (d) Optothermal-driven soft swimmer on the liquid–air interface. Adapted with permission from ref 56. Copyright 2019 American Association for the Advancement of Science. (e) Optothermal-driven Janus particle swimming in bulk fluid. Adapted with permission under a Creative Commons CC BY License from ref 38. Copyright 2020 Springer Nature. (f) Optothermal-driven asymmetric particle on liquid–air interface. Adapted with permission under a Creative Commons CC BY License from ref 57. Copyright 2015 Springer Nature. (g) Schematic of optothermal manipulation of particles for active matter research. Adapted with permission from ref 59. Copyright 2019 American Association for the Advancement of Science. (h) Schematic and optical image of a colloidal superstructure fabricated using

optothermal manipulation; From ref 60. Copyright The Authors, some rights reserved; exclusive licensee American Association for the Advancement of Science. Distributed under a CC BY-NC 4.0 license. Reprinted with permission from American Association for the Advancement of Science. Scale bar: 5 μm . (i) Schematic of optothermal manipulation used for plasmonic nanoparticle assembly and in situ surface-enhanced Raman spectroscopy. Adapted with permission from ref 63. Copyright 2017 American Chemical Society.

Author Manuscript

Author Manuscript

Author Manuscript

Author Manuscript

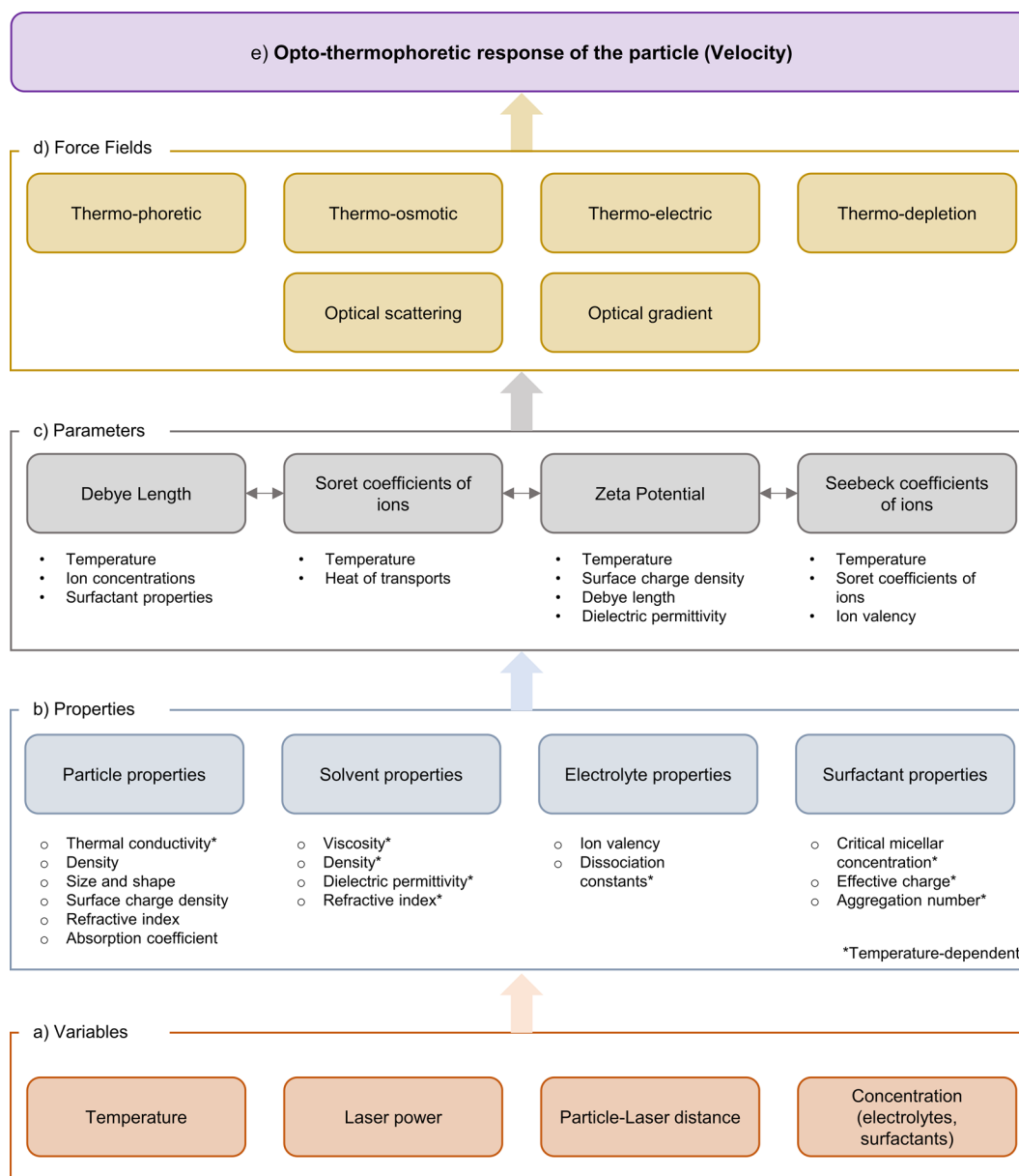


Figure 5. Modeling framework for obtaining the opto-thermophoretic response of a particle in a particular solution (a) Tunable variables include the ambient temperature of the solution, laser power, particle–laser distance, and the concentration of electrolytes/surfactants in the solution. (b) The particle’s response also depends strongly on several properties of the particle, solvent, electrolyte, and surfactant. Many properties are dependent on temperature. (c) Based on the variables and properties, other important parameters such as the Debye length and Seebeck effect are obtained. Several intricate dependences exist at this stage. (d) Different force fields that arise on the particle based on the properties are estimated. (e) Finally, the opto-thermophoretic response of the particle is evaluated using the net force on the particle.